large systems in an attempt to simulate the hydrogen bonding of formamide in dilute aqueous solution and in the liquid state. These represent only the first step in the construction of a theoretical model of these solutions. To obtain a more complete picture, statistical mechanical and thermodynamic treatments of these systems would certainly have to be made. Although the relationship between the model systems and the liquid state is crude, the results of the calculations seem to be significant since they do appear to be in reasonable agreement with experimental results and provide an insight into the bonding and structure not obtainable by experiment.

Acknowledgments. We wish to acknowledge Professor N. S. Ostlund for the use of his computer program required to make the calculations. We are indebted to Dr. A. Pullman for her very helpful discussions and suggestions. We wish to acknowledge the financial assistance provided by the Petroleum Research Fund, administered by the American Chemical Society, for partial support of this research and to NATO for a NATO Research Grant No. 1120. The authors are grateful to the University of Arkansas Computer Center for providing the necessary computing facilities.

References and Notes

(1) E. S. Amis and J. F. Hinton, "Solvent Effects on Chemical Phenomena", Vol. 1, Academic Press, New York, N.Y., 1973.
(2) J. A. Schellman, *C. R. Trav. Lab. Carlsberg*, **29**, 223 (1955).
(3) W. Kauzmann, *Adv. Protein Chem.*, **14**, 1 (1959).
(4) I. M. Klotz and J. S. Franzen, *J. Am. Chem. Soc.*, **84**, 3461 (1962).
(5) A. Johansson and P. A. Kollman, *J. Am. Chem. Soc.*, **94**, 6196 (1972).
(6) J. F. Hinton and K. H. Ladner, *J. Magn. Reson.*, **6**, 568 (1972).
(7) J. F. Hinton and C. E. Westerman, *Spectrochim. Acta, Part A*, **26**, 1387 (1970).
(8) J. F. Hinton, K. H. Ladner, and W. E. Stewart, *J. Magn. Reson.*, **12**, 90 (1973)
(9) J. E. Del Bene, *J. Chem. Phys.*, **62**, 1961 (1975).
(10) M. Dreyfus and A. Pullman, *Theor. Chim. Acta*, **19**, 20 (1970).
(11) M. Dreyfus, B. Maigret, and A. Pullman, *Theor. Chim. Acta*, **17**, 109 (1970).
(12) M. Dreyfus and A. Pullman, *C. R. Hebd. Seances Acad. Sci.*, **271**, 457 (1970).
(13) R. Janoschek, *Theor. Chim. Acta*, **32**, 49 (1973).
(14) T. Ottersen and H. J. Jensen, *J. Mol. Struct.*, **26**, 365 (1975).
(15) G. Alagona, A. Pullman, E. Scrocco, and J. Tomasi, *Int. J. Pept. Protein Res.*, **5**, 251 (1973).
(16) A. Johansson, P. Kollman, S. Rothenberg, and J. McKelvey, *J. Am. Chem. Soc.*, **96**, 3794 (1974).
(17) A. S. N. Murthy and C. N. R. Rao, *J. Mol. Struct.*, **6**, 253 (1970).
(18) T. Ottersen and H. J. Jensen, *J. Mol. Struct.*, **26**, 375 (1975).
(19) G. N. Port and A. Pullman, *I.I.Q.C. Quantum Biology Symposium*, **No. 1**, 21 (1974).
(20) J. Ladell and B. Post, *Acta Crystallogr.*, **7**, 559 (1954).
(21) S. Mizushima, "Structure of Molecules and Internal Rotation", Academic Press, New York, N.Y., 1954.
(22) H. Siegbahn, L. Asplund, P. KelFve, K. Hamrin, L. Karlsson, and K. Siegbahn, *J. Electron Spectrosc. Relat. Phenom.*, **5**, 1059 (1974).
(23) J. Del Bene and J. A. Pople, *J. Chem. Phys.*, **52**, 4858 (1970).
(24) D. Hankins, J. W. Moskowitz, and F. H. Stillinger, *J. Chem. Phys.*, **53**, 4544 (1970).
(25) H. Spiesecke and W. G. Schneider, *J. Chem. Phys.*, **35**, 731 (1961).
(26) G. E. Maciel and J. J. Natterstad, *J. Chem. Phys.*, **42**, 2427 (1965).
(27) G. C. Levy, G. L. Nelson, and J. D. Cargioli, *Chem. Commun.*, 506 (1971).
(28) W. R. Woolfenden and D. M. Grant, *J. Am. Chem. Soc.*, **88**, 1496 (1966).
(29) R. Lazzeretti and F. Taddei, *Org. Magn. Reson.*, **3**, 283 (1971).
(30) J. F. Sebastian and J. R. Grunwell, *Can. J. Chem.*, **49**, 1779 (1971).
(31) T. Tokuhiro and G. Fraenkel, *J. Am. Chem. Soc.*, **91**, 5005 (1969).
(32) W. Adams, A. Grimison, and G. Rodriquez, *Tetrahedron*, **23**, 2513 (1967).
(33) J. E. Bloor and D. L. Breen, *J. Am. Chem. Soc.*, **89**, 6835 (1967).
(34) G. A. Olah, P. W. Westerman, and D. A. Forsyth, *J. Am. Chem. Soc.*, **97**, 3419 (1975).
(35) H. Spiesecke and W. G. Schneider, *Tetrahedron Lett.*, 468 (1961).
(36) T. K. Wu and B. P. Dailey, *J. Chem. Phys.*, **41**, 2796 (1964).
(37) A. Veillard and B. Pullman, *C. R. Hebd. Seances Acad. Sci.*, **253**, 2418 (1961).
(38) V. Skala and J. Kuthan, *Collect. Czech. Chem. Commun.*, **35**, 2378 (1970).
(39) B. P. Dailey, A. Gawer, and W. C. Neikam, *Discuss. Faraday Soc.*, **No. 34**, 18 (1962).
(40) H. Gunther, J. Prestien, and P. Joseph-Nathan, *Org. Magn. Reson.*, **7**, 339 (1975).
(41) G. J. Martin, M. L. Martin, and S. Odiot, *Org. Magn. Reson.*, **7**, 1 (1975).
(42) T. Ottersen, *Acta Chem. Scand., Ser. A*, **29**, 939 (1975).

Electronic Structure and Proton Affinity of Methylenephosphorane by ab Initio Methods Including Electron Correlation

Hans Lischka

Contribution from the Institut für Theoretische Chemie und Strahlenchemie, Universitaet Wien, A-1090 Wien, Austria. *Received April 13, 1976*

Abstract: The electronic structures of methylenephosphorane PH_3CH_2 and its protonated adduct $PH_3CH_3^+$ were computed at the SCF level and with inclusion of electron correlation in the IEPA, CEPA, and PNO-CI schemes. For the equilibrium distance R_{PC} and the force constant k_{PC} we obtained the following values: PH_3CH_2, R_{PC}(SCF) = 3.16 au (1.67 Å), R_{PC}(CEPA) = 3.19 au (1.69 Å), k_{PC}(SCF) = 5.90 mdyn/Å, and k_{PC}(CEPA) = 5.53 mdyn/Å; $PH_3CH_3^+$, R_{PC}(SCF) = 3.42 au (1.81 Å), R_{PC}(CEPA) = 3.45 au (1.83 Å), k_{PC}(SCF) = 3.51 mdyn/Å, and k_{PC}(CEPA) = 3.25 mdyn/Å. The dipole moment μ(SCF) of PH_3CH_2 is 3.18 D. The proton affinitiy of PH_3CH_2 is in the SCF approximation −272.3 kcal/mol and −263.4, −267.9, and −269.7 kcal/mol in IEPA, CEPA, and PNO-CI, respectively The energy of the highest occupied MO agrees reasonably well with the lowest ionization energy of $(CH_3)_3PCH_2$. The properties of the molecular orbitals and the total electron density were investigated by means of contour diagrams and density plots. In agreement with experimental NMR and previous theoretical results we find the carbanion character in PH_3CH_2 dominating. Artifacts of the Mulliken population analysis and the arbitrariness of defining atomic radii are discussed. From a comparison of R_{PC} and k_{PC} calculated with different basis sets we conclude that a large amount of the shift in R_{PC} and k_{PC} going from $PH_3CH_3^+$ to PH_3CH_2 is due to the carbanion character of PH_3CH_2 without participation of any d functions. The remaining effects cannot be simply explained by a d_π–p_π bond in the highest occupied MO only.

The electronic structure of phosphorus ylides or alkylidene phosphoranes is generally formulated as a resonance hybrid of two structures:

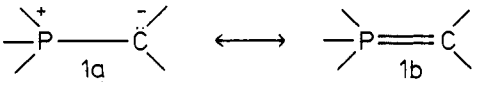

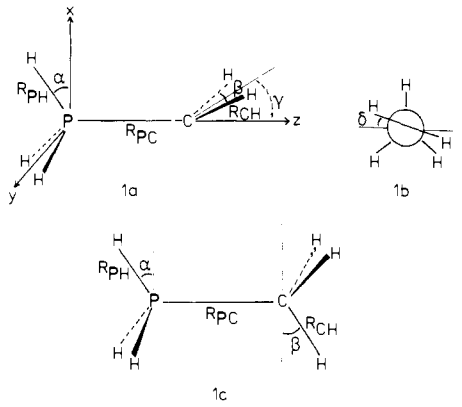

Figure 1. Definition of geometry parameters for PH_3CH_2 and $PH_3CH_3^+$.

^1H, ^{13}C, and ^{31}P NMR experiments[1-4] and ESR measurements[5] of corresponding radical cations have been interpreted to show a predominance of the structure **1a,** whereas the abnormally short P–C bond distances[6,7] favor the d_π–p_π double bond formulation **1b.** From infrared spectra of the nonstabilized ylides $(CH_3)_3PCH_2$ and $(Ph)_3PCH_2$ bond orders between 1.3 and 1.65 were deduced.[8,9] However, the interpretation of experimental data is complicated in many cases by the fact that the properties of the P–C bond are considerably modified by substitution effects.

Quantum chemical calculations are nowadays very well suited to supply interesting and sufficiently accurate information about the characteristics of chemical bonds. Semiempirical[10-12] calculations and one ab initio SCF investigation with medium sized basis sets[13] have been performed on the model substance PH_3CH_2 and a few of its derivatives for a very limited number of geometries.

In this work the geometry of PH_3CH_2 and its protonated adduct $PH_3CH_3^+$ is optimized with flexible basis sets at a near Hartree–Fock level and the effects of electron correlation on force constants and the barrier of rotation are calculated. Furthermore we discuss the electronic structure and the nature of the P–C bond on the basis of individual MO's and of the total electron density.

Method of Calculation

Starting from a conventional Hartree–Fock type SCF calculation the electron correlation energy is computed in the frameworks of IEPA (independent electron pair approximation), CEPA (coupled electron pair approximation), and PNO-CI (pair natural orbital CI). Among these approaches CEPA is regarded as the most reliable one for the evaluation of electron correlation effects. For further information about these methods see ref 14–18 and literature cited therein. The electron correlation energies are computed with reference to localized valence orbitals, which were obtained according to Boys criterion.[19] Only the valence shell electron correlation energy is calculated.

Basis Sets and Geometries

The Gaussian basis sets constructed from lobes as described in ref 20 are collected in Table I. The basis contains a 10s 6p set for P, a 8s 4p set for C, and a 3s set for each hydrogen atom, leaving the functions for the valence shell uncontracted. Since the highest occupied molecular orbital has carbanion character with a relatively diffuse electron density distribution, one set of s and p functions was added to the original 7s 3p set at the carbon atom. The corresponding orbital exponents were optimized keeping the exponents of the 7s 3p set fixed. This basis corresponds roughly to double ζ quality. The exponents of the

Table I. Basis Sets for PH_3CH_2 and $PH_3CH_3^+$

No.	Atom	Primitive set	Contraction	Exponent	Ref
1	P	10s 6p	(511111/3111)		*a*
	C	7s 3p	(4111/21)		*a*
		1s 1p		0.1/0.06	
	H_P[e]	3s[c]	(21)		*b*
	H_C[f]	3s[d]	(21)		*b*
2[g]	P	d_{xz}		0.5	
3[g]	P	1d		0.5	
4[g]	C	1d		0.3	
5[g]	P	1d		0.5	
	C	1d		0.3	
	H_P	1p		0.55	
	H_C	1p		0.75	
6[h]	P	2d		0.5/1.5	
7[h]	C	2d		0.2/0.6	

[a] S. Huzinaga, "Approximate Atomic Functions", University of Alberta, Canada, 1971. [b] S. Huzinaga, *J. Chem. Phys.*, **42,** 1293 (1965). [c] Scaled by a factor 1.69. [d] Scaled by a factor 1.44. [e] Hydrogen atoms bonded to phosphorus. [f] Hydrogen atoms bonded to carbon. [g] The basis sets No. 2–5 are derived from basis No. 1 by addition of the functions indicated. [h] The remaining basis functions are the same as those of basis No. 5.

polarization functions optimized at the SCF level are shown for the basis sets 2–7. Since they agree quite well with previous optimizations of IEPA energies[21,22] we did not reoptimize the exponents for the correlation energy calculations. Only the exponent of the d function at the carbon atom is significantly smaller than that for CH_4 in ref 21, which is due to the aforementioned partial carbanion character.

The investigated geometries and the coordinate system are described in Figure 1. Beginning with a reasonable guess of starting values, the geometry parameters were chain optimized and the procedure terminated after completion of the first cycle. During all our calculations the local C_{3v} symmetry at the carbon atom in $PH_3CH_3^+$ and at phosphorus was preserved.

Results

Some numerical results of our SCF and correlation energy calculations are collected in Table II. Table III shows geometries, the force constants k_{PC}, and the dipole moment μ. The PC bond distance in PH_3CH_2 is somewhat larger than 3.14 au obtained for $(Ph)_3PCH_2$,[7] demonstrating the stabilizing effect of the phenyl substituents. The IR spectrum of trimethylmethylenephosphorane has been analyzed in detail.[9] The resulting 5.59 mdyn/Å for the force constant k_{PC} is in good agreement with our value. The effect of electron correlation on distances and force constants is smaller than in the cases of N_2 and F_2.[23] As to be expected, R_{PC} in $PH_3CH_3^+$ is increased with respect to PH_3CH_2 but smaller than the sum of the single bond radii of phosphorus and carbon (3.54 au).[24] R_{PH} in PH_3CH_2 is less than in pyramidal PH_3 (2.685 au)[25] and is still more contracted in $PH_3CH_3^+$. We find the CH distance in PH_3CH_2 shorter than the respective value for C_2H_4 (2.05 au)[25] but close to the value 2.033 au in planar CH_3^-.[26] However, R_{CH} is significantly larger than the value 1.80 au assumed by Absar and Van Wazer.[13]

The out-of-plane angle α of the PH_3 group is reduced to a near tetrahedral angle in $PH_3CH_3^+$. A slight distortion from planarity of the PCH_2 arrangement is shown by $\gamma = 10°$, $\delta = 0°$ in PH_3CH_2. Two points were calculated for $\delta = 90°$ (eclipsed conformation of PH_3CH_2), which show $\gamma = 0°$ most stable. In agreement with the calculations by Absar and Van Wazer,[13] the barrier of rotation for PH_3CH_2 is practically zero at the SCF level as well as with inclusion of electron correlation

Table II. SCF and Correlation Energies Obtained with Basis No. 5 for Some Selected Geometries of PH_3CH_2 and $PH_3CH_3^+$ [a]

	R_{PC}	γ, deg	δ, deg	$-E_{SCF}$	$-E_{CORR}$ IEPA	$-E_{CORR}$ CEPA	$-E_{CORR}$ PNO-CI	$-E_{tot}$ IEPA	$-E_{tot}$ CEPA	$-E_{tot}$ PNO-CI
Ph_3CH_2	3.20	0	0	381.263 704	0.354 999	0.304 791	0.271 994	381.618 702	381.568 494	381.535 698
	3.20	0	45	381.263 728	0.354 908	0.304 695	0.271 912	381.618 635	381.568 423	381.535 640
	3.20	0	90	381.263 698	0.354 894	0.304 705	0.271 914	381.618 592	381.568 403	381.535 612
	3.14	−10	0	381.263 592						
	3.14	0	0	381.263 893						
	3.14	10	0	381.264 001						
	3.14	20	0	381.263 868						
	3.14	0	90	381.263 887						
	3.14	10	90	381.263 790						
$Ph_3CH_3^+$	3.45	Staggered		381.697 739	0.340 627	0.297 596	0.267 681	382.038 365	381.995 334	381.965 419
	3.45	Eclipsed		381.694 879	0.340 540	0.297 577	0.267 643	382.035 419	381.992 456	381.962 522

[a] All values are in au. The values of the geometry parameters not shown are those given in Table III. For a defintion of bond distances and angles see Figure 1.

Table III. Geometry and Force Constants k_{PC} for the PH_3CH_2 and $PH_3CH_3^+$ Molecules Obtained with Basis No. 5[a]

	PH_3CH_2	$PH_3CH_3^+$
R_{PC} SCF	3.16	3.42
CEPA	3.19	3.45
R_{PH}	2.65	2.64
R_{CH}	2.025	2.06
α, deg	28	22
β, deg	121	20
γ, deg	10	
k_{PC} SCF	5.90	3.51
CEPA	5.53	3.25
μ(SCF) and Cartesian components	3.18 (0.10, 0, 3.17)	

[a] The force constants are given in mdyn/Å, the dipole moment in D, the bond distances in au. For a definition of geometry parameters see Figure 1. δ was fixed at 0° (staggered conformation).

Table IV. Basis Set Dependence of the SCF Energy for PH_3CH_2[a]

Basis No.	$-E_{SCF}$, au	Basis No.	$-E_{SCF}$, au
1	381.140 280	5	381.263 893
2	381.179 514	6	381.275 630
3	381.229 957	7	381.266 815
4	381.160 130		

[a] R_{PC} = 3.14 au, γ = 0°. The values of the remaining geometry parameters are those shown in Table III.

(cf. the first three lines in Table II). This is also exemplified by the near constancy of the orbital energies (see below). For $PH_3CH_3^+$ the barrier is much larger: SCF, 0.002 86 au; IEPA, 0.002 95 au; CEPA 0.002 88 au; PNO-CI 0.002 90 au. Since no independent geometry optimization for the eclipsed conformation was performed, a slight modification of these values is still to be expected. For reasons of computational economy the calculations of the force constants and all further investigations were performed with γ = 0° and δ = 0° for PH_3CH_2 and the staggered conformation of $PH_3CH_3^+$.

At the SCF level we obtain −272.3 kcal/mol for the proton affinity of PH_3CH_2, which is reduced to −263.4, −267.9, and −269.7 kcal/mol in IEPA, CEPA, and PNO-CI, respectively. The proton affinity is thus intermediate between the value of the C=C bond in C_2H_4 (SCF, −174.7 kcal/mol; IEPA, −160.2 kcal/mol)[27] and that for CH_3^- (SCF, −433.5 kcal/mol; IEPA, −420.3 kcal/mol.[21,26]

The dipole moment is relatively large, indicating the polarity of methylenephosphorane. To our knowledge experimental data exist only for stabilized ylides[28-30] (5.5–7 D). They cannot be compared directly with our results because of additional substitution effects. We find the orbital sequence for the staggered conformation (valence orbitals only) 6a′, 7a′, 2a″, 8a′, 9a′, 3a″, and 10a′ and the respective orbital energies (in eV, basis No. 5) −26.51, −21.88, −16.20, −15.46, −14.44, −14.02, and −7.40. This sequence was also obtained by Absar and Van Wazer.[13] Since these authors also characterized the individual MO's with respect to bonding and antibonding properties, we need not further comment on this point. Their orbital energy of −7.20 eV for the highest occupied MO (HOMO) is close to our value. However, much larger deviations (0.5–0.8 eV) exist for the orbitals 6a′, 7a′, and 8a′. It should be noted that the effect on the 10a′ MO by adding a p set with exponent 0.06 (see Table I) to the 7s 3p basis is even larger than the total residual change by all the polarization functions. Addition of one d set on phosphorus lowers ϵ(10a′) by ~0.3 eV but overshoots the final orbital energy by ~0.1 eV. This overshooting is even more pronounced in the Mulliken population analysis (see next section). As mentioned above, the orbital energies remain practically constant up to four figures upon rotation of the CH_2 group from the staggered to the eclipsed conformation (δ = 0, 45, 90°). The photoelectron spectrum has been observed for $(CH_3)_3PCH_2$.[12a] The lowest ionization potential is found at 6.87 eV. Considering the approximative character of Koopmans' theorem and the fact that the methyl groups certainly destabilize the ylidic structure due to inductive effects, the agreement is reasonable. In semiempirical calculations the energy of the 10a′ MO is too low and the stabilizing effect of the d orbitals on phosphorus is strongly exaggerated (CNDO/2, ϵ(10a′) = −12.22 eV with d orbitals, −9.36 eV without d orbitals;[12a] the corresponding numbers obtained by an extended Hückel treatment are −12.39 and −11.20 eV[10]).

SCF energies for the different basis sets are listed in Table IV. Without polarization functions (basis No. 1) we arrive at a value which is ~0.3 au below that of the previous SCF calculations by Absar and Van Wazer,[13] showing the superior flexibility of our s and p basis. The effect of a single d_{xz} function on phosphorus, which should be capable of d_π–p_π bonding, introduces only half of the energy gain of the complete d set. Inclusion of a d set on P brings about four times as much in energy as a d set on C. The second d set is also more important for phosphorus than for carbon (basis No. 6 and 7). Considering the truncation error of the atomic basis set and the Hartree–Fock limit of PH_3,[22] we estimate from Table IV the Hartree–Fock limit of PH_3CH_2 to be −381.440 au and, accordingly, 14.5 eV for the Hartree–Fock binding energy. An

Table V. IEPA Pair Correlation Energies for PH_3CH_2 and $PH_3CH_3^+$ from Localized Orbitals[a] with Basis No. 5[b]

	Intrapair				Interpair[c]						
	$-\epsilon_{PH}$	$-\epsilon_{PC}$	$-\epsilon_{HOMO}$	$-\epsilon_{CH}$	$-\epsilon_{PH,PH'}$	$-\epsilon_{PH,PC}$	$-\epsilon_{PH,HOMO}$	$-\epsilon_{PC,HOMO}$	$-\epsilon_{PC,CH}$	$-\epsilon_{HOMO,CH}$	$-\epsilon_{CH,CH'}$
PH_3CH_2	0.02700	0.01934	0.02080	0.02669	0.00828	0.00761	0.00570	0.02674	0.01194	0.02353	0.01215
$PH_3CH_3^+$	0.02883	0.02217		0.02750	0.00891	0.00854			0.01485		0.01485
CH_3^- [26]			0.0264[d]	0.0292							0.01371
C_2H_4 [23]			0.0333[e]	0.0299							0.01384
PH_3 [22]	.0286				0.0095						

[a] Only the orbitals 6a′–3a″ of staggered PH_3CH_2 were transformed, resulting in one unique and two equivalent PH bonds, one PC and two equivalent CH bonds. The HOMO was not modified by the localization procedure. A mean value for the contributions of the three PH bonds is given. In the case of $PH_3CH_3^+$ all valence orbitals were transformed. [b] Geometry: PH_3CH_2, R_{PC} = 3.20 au, γ = 0°; $PH_3CH_3^+$, R_{PC} = 3.45 au, staggered conformation. The values of the remaining geometry parameters are those shown in Table III. [c] Sum of the singlet and triplet interpair contributions. [d] Lone pair correlation energy ϵ_n. [e] π orbital correlation energy ϵ_π.

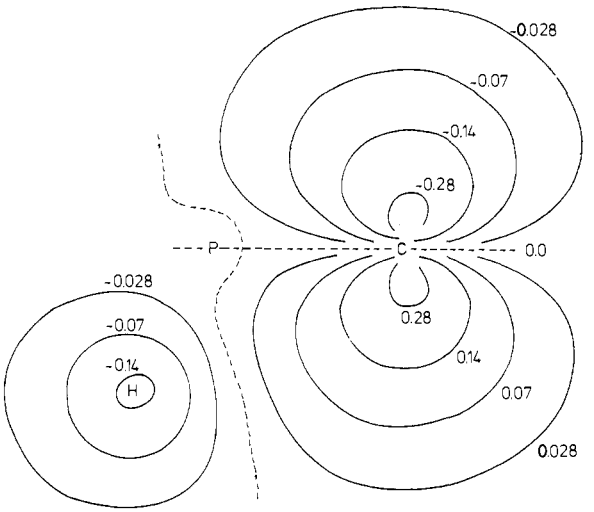

Figure 2. Contour lines (in au) of the 10a′ MO of PH_3CH_2 in the xz plane with basis No. 1.

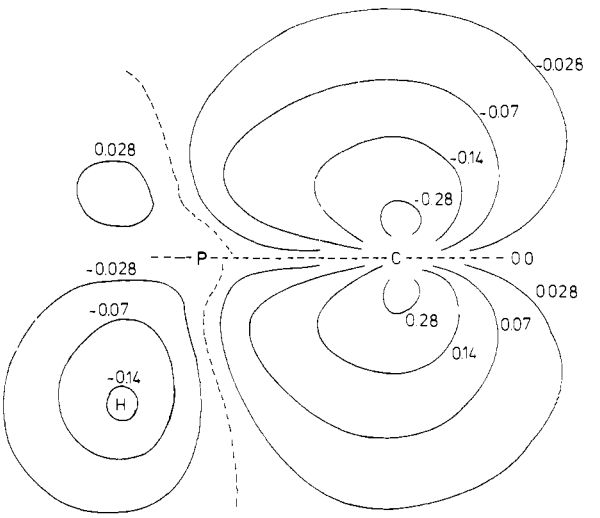

Figure 3. Contour lines (in au) of the 10a′ MO of PH_3CH_2 in the xz plane with basis No. 5.

analogous consideration leads to −381.875 au for the Hartree–Fock limit of $PH_3CH_3^+$.

In order to characterize the individual pair electron contributions, the IEPA results are documented in Table V together with results from reference molecules. The intrapair contributions are generally 10–15% smaller in absolute value than the corresponding energies of PH_3,[22] CH_3^-,[26] and C_2H_4.[23] Only $|\epsilon_{HOMO}|$ is significantly smaller than the respective pair correlation energies of CH_3^- and C_2H_4. However, a pilot calculation with basis No. 7 (2 d sets on C) for ϵ(10a′) gave −0.022 55 au. We thus expect that about 50–60% of the valence shell correlation energy is covered by our calculations. In keeping with the results for the second-row hydrides[22] we find $|\epsilon_{PH,PH}|$ significantly smaller than the interpair contributions of the first-row hydrides. Because of the large separation of the PH and CH bond orbitals in space, $|\epsilon_{PH,CH}|$ is of the order of magnitude of ~0.001 au and therefore not included in Table V. The dominating interpair energies in PH_3CH_2 are $\epsilon_{PC,HOMO}$ and $\epsilon_{HOMO,CH}$, involving the ylidic HOMO. Their modification on protonation is mainly responsible for the reduction of the electron correlation energy (in absolute value) in $PH_3CH_3^+$ vs. PH_3CH_2. The importance of the interpair contribution to dimerization and protonation processes has already been demonstrated for BH_3[31] and C_2H_4.[27]

Interpretation of Molecular Orbitals and Electron Densities

Since most discussions concerning the character of the PC bond in ylides start with the interpretation of the HOMO (10a′ MO) we first concentrate on this orbital. In Figure 2 the contour map of the 10a′ orbital is displayed in a basis without any polarization functions (basis No. 1). We observe an essentially p-type orbital on carbon (see also Figure 2 in ref 13) with minor contributions in the region of the hydrogens bonded to phosphorus. Figure 3 demonstrates the effect of a complete polarization set (basis No. 5). Comparing Figures 2 and 3 no dramatic changes can be observed by the addition of a d set on phosphorus. However, such changes should be expected, if a d_π–p_π double bond was formed. The effect of both d sets (on carbon and phosphorus) is rather polarization of the p orbital toward phosphorus. On the other hand one should stress that the p orbital itself extends far into the bonding region, as is demonstrated perhaps more clearly by the integrated electron density diagrams later in this section. Figure 4 shows the 10a′ orbital in a plane parallel to the yz plane at x = −0.6 au. From this figure we conclude that its orbital density also extends into the region of the hydrogen atoms of the CH_2 group. The consequences will be discussed in connection with the population analysis.

The localization of molecular orbitals is not unique. Up to now the 10a′ orbital has been excluded from the localization procedure (see Table V, footnote *a*). We now present for further illustration in Figure 5 the two localized orbitals belonging to the PC bond region when mixing between all valence orbitals is allowed. In ethylene there result two "banana bonds" symmetrically above and below the molecular plane.[32] In our case the drawings resemble rather two strongly distorted p-type functions on carbon being continued on opposite sides into the vicinity of phosphorus. We abandoned the further use of this type of localization and kept in the following discussion the original type of localization separating the 10a MO from the remaining orbitals.

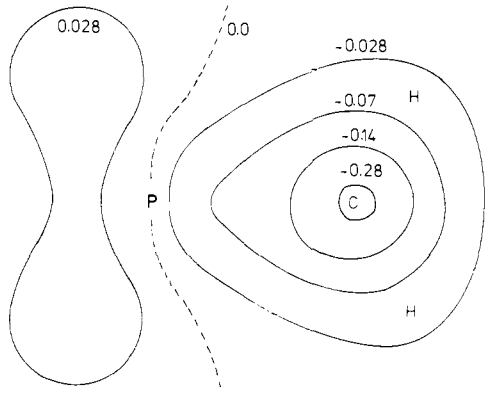

Figure 4. Contour lines (in au) of the 10a′ MO of PH_3CH_2 in the plane parallel to the yz plane ($x = -0.6$ au) with basis No. 5.

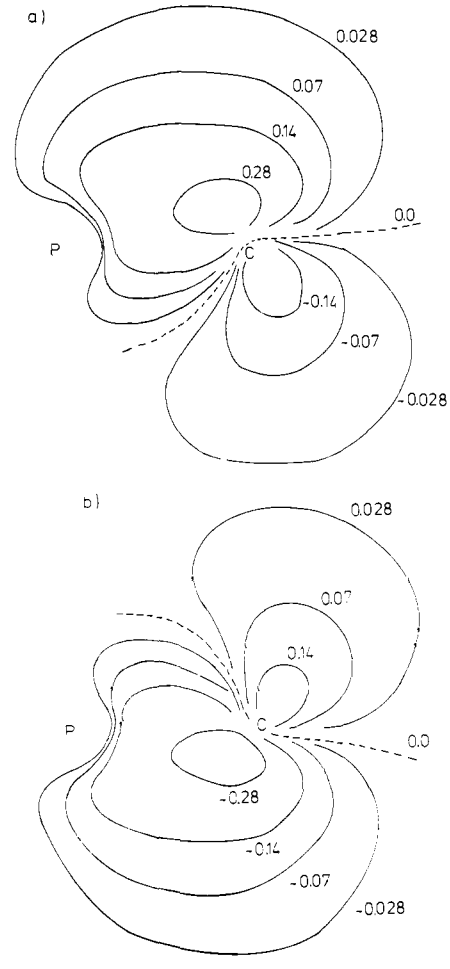

Figure 5. Contour lines (in au) of the two "banana bond"-type localized MO's in the xz plane with basis No. 5.

Table VI shows how the gross atomic populations according to the Mulliken analysis[33] change with variation of the basis. From the analysis of the 10a′ orbital alone we find most of the density concentrated around the carbon atom, a minor amount of charge situated on phosphorus, and practically nothing on the hydrogens H_C. As one would expect, the effect of the d set on phosphorus is to increase its charge. Including the complete polarization set (basis No. 5) the effect is somewhat diminished. The changes with different basis sets are much more pronounced in the case of the total density. Especially the inclusion of the d set on carbon reduces the charge on phosphorus drastically and increases the population on C. Surprisingly, this effect on phosphorus is not counterbalanced but rather enhanced by the complete polarization set. The decrease of charge on carbon is not transferred to phosphorus but to the hydrogen atoms. Among the contribution from the d set on P the d_{xz} part dominates, but the sum of the remaining d functions is even larger.

In the last columns in Table VI previous results are collected. The charges on carbon from our calculation are larger by ~0.2 e_0 than those obtained by the ab initio calculation of Absar and Van Wazer.[13] This is probably due to our additional p set on carbon with exponent 0.06. Table VI very clearly shows the difficulties in obtaining formally well balanced basis sets.[34] The main reasons for these difficulties are not to be located in the highest occupied 10a′ orbital but in the remaining MO's.

In order to avoid the effect of basis set imbalance on the population analysis, we regard directly the electron density function $\rho(x, y, z)$. Since we are mainly discussing the details along the PC bond (in the z direction), the density function is integrated over the x and y coordinates:

$$\rho(z) = \int_{-\infty}^{\infty} \int_{-\infty}^{\infty} \rho(x, y, z)\, dx\, dy$$

In this case it is easy to define atomic radii by means of integration limits z_i along the z axis and to attribute the resulting integrated charge densities

$$\rho_i = \int_{z_i}^{z_{i+1}} \rho(z)\, dz$$

to the respective atoms. This procedure is best suited for linear molecules, but we believe that the main features we are interested in are quite well reproduced. Naturally, the arbitrariness in dividing up the electron charge density in the bonding region cannot be removed. In order to test the effect of different boundaries between P and C we employed two choices: (a) the location of the minimum of the electron density $\rho(z)$ (PH_3CH_2, $z_{min} = 1.26$ au; $PH_3CH_3^+$, $z_{min} = 1.75$ au) and (b) the double bond and single bond radii of phosphorus given by Pauling[24] (PH_3CH_2, $z_{cov} = 1.89$ au; $PH_3CH_3^+$, $z_{cov} = 2.08$ au). The projection of the covalent radii along the PH and CH bonds onto the z axis served as definition for boundaries between P and H and C and H, respectively. The minimum of the electron density has also been used by Bader et al.[35] for the calculation of atomic charges in their extended investigation of linear molecules. In connection with the interpretation of the electronic structure of intermolecular complexes Schuster et al.[36] evaluated the effect of different boundary definitions on charge transfer.

The atomic charges are collected in Tables VII and VIII. Δ_{PC} is the charge density integrated between z_{min} and z_{cov} and serves as a measure for the abovementioned arbitrariness. Figures 6 and 7 show plots of $\rho(z)$ for the 10a′ and σ_{PC} orbitals of PH_3CH_2 in the localized description.

From Figure 6 and Table VII we find in agreement with the population analysis that the main portion of the charge density of the 10a′ orbital is situated around the carbon atom. The variation of the basis shows the expected effects. But there is one essential difference to the results of the population analysis: as was already indicated by the contour diagram (Figure 4) a charge of ~0.15 e_0 is attributed to each of the hydrogens H_C. The reason why the Mulliken population analysis is unable to reproduce this behavior lies in the fact that the functions creating charge density at the hydrogens are formally situated on the carbon atom. But it is essentially this shielding effect which is responsible for the high-field shift of the NMR absorption lines of the methylene protons.[37] Another interesting feature is shown in Table VII. Δ_{PC} is relatively small for the 10a′ orbital (~0.15 e_0) but much larger (~0.5 e_0) for the σ_{PC}

Table VI. Mulliken Gross Atomic Populations for PH_3CH_2

	Basis No.	10a′ 1	10a′ 3	10a′ 4	10a′ 5	Total density 1	Total density 3	Total density 4	Total density 5	Absar and Van Wazer[13] No d	Absar and Van Wazer[13] With d	EHT[10] No d	EHT[10] With d	CNDO/2[12a] No d	CNDO/2[12a] With d
P	s					5.40	5.40	5.29	5.08						
	p_x	0.04	0.04	0.03	0.03	3.01	3.01	2.99	2.83						
	p_y					2.95	2.93	2.94	2.78						
	p_z					2.97	3.03	2.75	2.79						
	d_{z^2}						0.05		0.03						
	d_{xz}		0.12		0.10		0.14		0.12						
	d_{yz}						0.06		0.05						
	$d_{x^2-y^2}$		0.01				0.04		0.03						
	d_{xy}						0.03		0.02						
Σ		0.04	0.17	0.03	0.13	14.34	14.68	13.97	13.74	14.49	14.89	14.25	14.84	14.34	14.66
C	s					3.32	3.22	3.53	3.28						
	p_x	1.65	1.60	1.68	1.60	1.72	1.66	1.75	1.67						
	p_y					1.26	1.21	1.24	1.07						
	p_z					0.87	0.84	1.12	1.01						
	d_{z^2}							0.03	0.02						
	d_{xz}			0.01	0.01			0.01	0.02						
	d_{yz}								0.01						
	$d_{x^2-y^2}$							0.02	0.01						
	d_{xy}														
Σ		1.65	1.60	1.69	1.61	7.16	6.94	7.68	7.10	6.94	6.68	7.07	6.51	6.46	6.30
H_P	s	0.20	0.15	0.19	0.14	1.05	0.99	1.04	1.13						
	p_x								0.03						
	p_y														
	p_z								0.01						
Σ		0.20	0.15	0.19	0.14	1.05	0.99	1.04	1.17	1.05	0.97	0.97	0.98	1.08[a]	1.06[a]
H_P'	s	0.05	0.04	0.05	0.04	0.99	0.94	0.99	1.09						
	p_x								0.01						
	p_y								0.02						
	p_z								0.01						
Σ		0.05	0.04	0.05	0.04	0.99	0.94	0.99	1.13	0.97	0.92	0.94	0.94		
H_C	s					0.74	0.76	0.66	0.83						
	p_x				0.01				0.01						
	p_y								0.02						
	p_z								0.01						
Σ					0.01	0.74	0.76	0.66	0.87	0.79	0.81	0.92	0.89	0.98	0.93

[a] Mean value for all hydrogens of the PH_3 group.

Table VII. Partitioning of the Integrated Charge Density $\rho(z)$ for PH_3CH_2[a]

Basis No.	Orbital	q_P	Δ_{PC}	q_C	q_{H_P}	q_{H_C}
1	σ_{PC}	0.63	0.49	0.74	0.02	0.03
	10a′	0.12	0.11	1.22	0.07	0.17
3	σ_{PC}	0.59	0.53	0.77	0.02	0.03
	10a′	0.18	0.15	1.18	0.06	0.16
4	σ_{PC}	0.61	0.53	0.75	0.02	0.02
	10a′	0.12	0.13	1.25	0.07	0.14
5	σ_{PC}	0.58	0.54	0.78	0.02	0.03
	10a′	0.17	0.16	1.20	0.06	0.14
1	Total	13.80	0.78	6.10	1.02	1.13
3	density	13.82	0.84	6.05	1.01	1.13
4		13.79	0.83	6.13	1.01	1.11
5		13.82	0.85	6.08	1.00	1.11

[a] σ_{PC} stands for the localized PC σ bond orbital.

Table VIII. Partitioning of the Integrated Charge Density $\rho(z)$ for $PH_3CH_3^+$ and Gross Atomic Population[a]

Basis No.	Orbital	q_P	Δ_{PC}	q_C	q_{H_P}	q_{H_C}
		$\rho(z)$				
1	σ_{PC}	0.89	0.22	0.70	0.03	0.04
5	σ_{PC}	0.88	0.25	0.72	0.02	0.03
1	Total	13.99	0.32	5.82	1.00	0.96
	density					
5		14.00	0.34	5.84	0.99	0.94
		Population Analysis				
1	Total	14.46		6.88	0.88	0.68
	density					
	5	13.82		6.74	1.03	0.79

[a] σ_{PC} stands for the localized PC σ bond orbital.

orbital, since in the latter case the electron density is concentrated in the bond region.

From the analysis of the total density we therefore obtain $\Delta_{PC} \sim 0.8$ e_0 demonstrating the wide range for the definition of atomic charges. But since we are particularly interested in the character of the 10a′ orbital, where Δ_{PC} is only ~ 0.15 e_0, and not so much in the details of the σ_{PC} bond, the carbanion character of the HOMO is well established. It is also generally assumed that trends in a series of calculations with the same choice of the atomic radii are reproduced more reliably than the absolute values of the atomic charges themselves. Δ_{PC} is much smaller for $PH_3CH_3^+$, since in this case z_{min} is situated closer to z_{cov} than for PH_3CH_2.

The basis set dependence is found to be much less pronounced in Table VII than it was in the case of the population analysis. Dividing Δ_{PC} arbitrarily in equal parts to P and C we

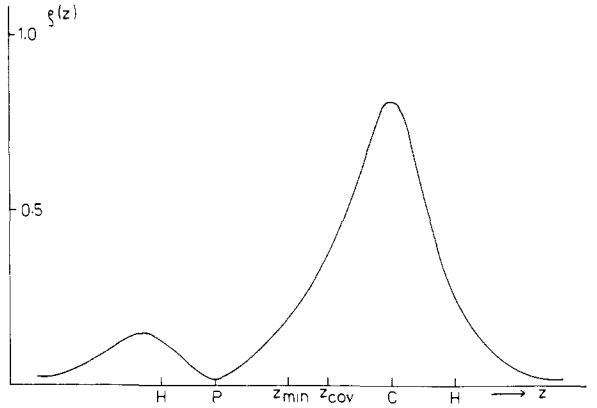

Figure 6. The integrated density function $\rho(z)$ (in au) for the 10a′ MO of PH_3CH_2 with basis No. 5. The projections of the atomic nuclei onto the z axis are shown. For definition of the atomic radii z_{min} and z_{cov} see text.

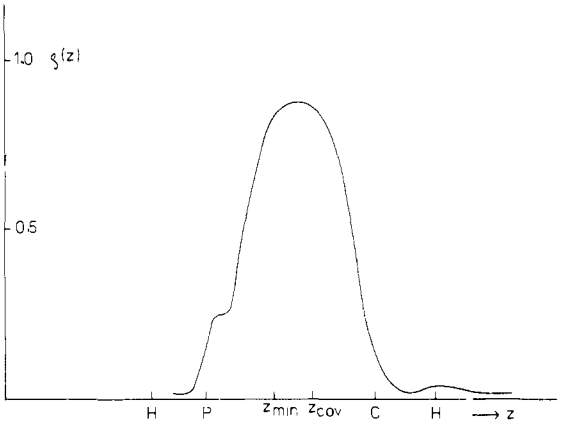

Figure 7. The integrated density function $\rho(z)$ (in au) for the σ_{PC} MO of PH_3CH_2 in the localized description with basis No. 5. The projections of the atomic nuclei onto the z axis are shown. For the definition of the atomic radii z_{min} and z_{cov} see text.

Table IX. Basis Set Dependence of the Force Constant k_{PC} (mdyn/Å) and the Equilibrium Distance R_{PC} (au) in the SCF Approximation

Basis No.	k_{PC}	R_{PC}
	PH_3CH_2	
1	4.142	3.279
2	5.018	3.189
3	5.905	3.153
4	5.010	3.220
5	5.897	3.161
	$PH_3CH_3^+$	
1	2.644	3.561
5	3.505	3.424

obtain a dipolar, though less extreme charge distribution than from the population analysis. The total charge on H_C is increased with respect to the results of Table VI due to the effects of the 10a′ orbital. We now obtain a negative net charge on H_C.

On protonation of PH_3CH_2 the most significant changes occur in the CH_2 fragment and the electron distribution around phosphorus is not much affected. This is in agreement with the interpretation of ^{31}P chemical shifts.[3] As one can infer from a comparison of Tables VII and VIII the charge on carbon is reduced, since the 10a′ orbital of PH_3CH_2 is utilized for an additional σ CH bond in $PH_3CH_3^+$. The charge on the H_C's decreases also. The results of the population analysis at the bottom of Table VIII exhibit again a much too large charge separation.

Charge densities and atomic populations are only one possibility to characterize chemical bonds. Additional information is obtained from infrared data about the shape of the potential energy curve near the energy minimum. It was already stated in the introduction that the abnormally short bond distance and the relatively large force constant were interpreted to favor the d_π–p_π double bond formalism **1b.** This view does not conform to NMR and ESR data and also not to our and previous theoretical results. It is therefore interesting to investigate the effect of d functions on force constant and equilibrium distance. In Table IX our results are collected.

Comparison of k_{PC} and R_{PC} for $PH_3CH_3^+$ in Table IX with the corresponding values in PH_3CH_2 shows that a large part of the shift is already achieved without any polarization functions (basis No. 1). The addition of a single d_{xz} on P, capable of d_π–p_π bonding, changes k_{PC} further in the correct direction. R_{PC} is quite close to R_{PC} calculated with basis No. 5. But nearly the same effect results by adding a d set on carbon (basis No. 4)! The complete d set on phosphorus (basis No. 3) overshoots the correct values slightly. A more complicated situation than d_π–p_π bonding alone was also shown to exist in the previous ab initio[13] and EHT[10] investigations. But in addition we find that the d set on phosphorus as well as the d set on carbon have significant influence on the potential energy curve.

Conclusions

The properties of the PC bond in methylenephosphorane and in its protonated adduct have been discussed from several points of view. From contour diagrams and density plots of the highest occupied (10a′) MO of PH_3CH_2 carbanion character is found in agreement with NMR data. The electron density of this MO is of course not concentrated exclusively in the immediate neighborhood of the carbon atom but extends into the bond region toward phosphorus and includes as well the hydrogen atoms of the CH_2 group. The contribution of d orbitals is significant, but their effect is polarization and not formation of a d_π–p_π double bond.

The possibility of d_σ bonding was investigated by Keil and Kutzelnigg[38] for the bipyramidal structure of PH_3F_2. The authors find from their SCF calculations that PH_3F_2 is stable without the participation of any d AO's on P. This result is in some respect similar to ours; the main features of the bond properties are reproduced in these cases already by the s and p basis set, but the d functions are necessary for a correct quantitative description. In order to obtain a balanced basis set one should use a complete set of polarization functions including also d orbitals on carbon.

The artifacts of the Mulliken population analysis were discussed. Basis effects are overestimated and the charges on the methylene protons are not reproduced correctly. The arbitrariness of defining atomic charges has been investigated by choosing different values for the atomic radii of P and C. We have found that the main source of uncertainty is due to the PC σ bond and thus does not affect our conclusions regarding the properties of the 10a′ MO. The major part of the decrease of R_{PC} and a large part of the increase of k_{PC} in PH_3CH_2 with respect to the corresponding values in $PH_3CH_3^+$ is due to the carbanion character. Thus, Coulomb forces resulting from the charge separation $P^{\delta+}$–$C^{\delta-}$ and the penetration of electron density of the HOMO into the bond region are shown to be important contributions to bond formation in ylides. d_π–p_π

double bond character in the HOMO accounts only in part for further changes of R_{PC} and k_{PC}. Other significant contributions come from the complete d set on carbon and the remaining d functions on phosphorus. It is of course possible to calculate bond orders in a formal sense from force constants and bond distances.[8,9,39] But, as it was shown in this work, the situation is much too complicated in the case of methylenephosphorane (and certainly also in other cases of similar types of bonding) to allow the interpretation of such bond orders in the simple scheme of d_π–p_π bonding according to structure **1b.**

Acknowledgment. The calculations were performed on the CDC CYBER 73/74 of the computer centers of the University and the Technical University of Vienna. We are grateful for sufficient supply of computer time and thank the staff of both centers for their cooperation. The computer program for plotting the orbital contour diagrams has been written by F. Keil, Karlsruhe/F.R.G.

References and Notes

(1) A. W. Johnson, "Ylid Chemistry", Academic Press, New York, N.Y., 1966, pp 76–79.
(2) A. J. Speziale and K. W. Ratts, *J. Am. Chem. Soc.*, **85**, 2790 (1963).
(3) S. O. Grim, W. McFarlane, and T. J. Marks, *Chem. Commun.*, 1191 (1967).
(4) H. Schmidbaur, W. Buchner, and D. Schentzow, *Chem. Ber.*, **106**, 1251 (1973).
(5) E. Lucken and C. Mazeline, *J. Chem. Soc. A*, 1074 (1966); 439 (1967).
(6) P. J. Wheatley, *J. Chem. Soc. A*, 5785 (1965).
(7) J. C. Bart, *J. Chem. Soc. B*, 350 (1969).
(8) W. Luttke and K. Wilhelm, *Angew. Chem.*, **77**, 867 (1965).
(9) W. Sawodny, *Z. Anorg. Allg. Chem.*, **368**, 284 (1969).
(10) R. Hoffmann, D. B. Boyd, and St. Z. Goldberg, *J. Am. Chem. Soc.*, **92**, 3929 (1970).
(11) D. B. Boyd and R. Hoffmann, *J. Am. Chem. Soc.*, **93**, 1064 (1971).
(12) (a) K. A. Starzewski, H. T. Dieck, and H. Bock, *J. Organomet. Chem.*, **65**, 311 (1974); (b) J. M. F. van Dijk and H. M. Buck, *Recl. Trav. Chim. Pays-Bas*, **93**, 155 (1974); (c) B. Klabuhn, *Tetrahedron*, **30**, 2327 (1974).
(13) I. Absar and J. R. Van Wazer, *J. Am. Chem. Soc.*, **94**, 2382 (1972).
(14) O. Sinanoglu, *Adv. Chem. Phys.*, **6**, 315 (1964).
(15) R. K. Nesbet, *Phys. Rev.*, **155**, 51 (1967).
(16) W. Meyer, *Int. J. Quantum Chem. Symp.*, **5**, 59 (1971).
(17) W. Meyer, *J. Chem. Phys.*, **58**, 1017 (1973).
(18) R. Ahlrichs, H. Lischka, V. Staemmler, and W. Kutzelnigg, *J. Chem. Phys.*, **62**, 1225 (1975).
(19) S. F. Boys, "Quantum Theory of Atoms, Molecules and the Solid State", P. O. Löwdin, Ed., Interscience, New York, N.Y., 1967, p. 253.
(20) R. Ahlrichs and F. Driessler, *Chem. Phys. Lett.*, **23**, 571 (1973).
(21) R. Ahlrichs, F. Driessler, H. Lischka, V. Staemmler, and W. Kutzelnigg, *J. Chem. Phys.*, **62**, 1235 (1975).
(22) R. Ahlrichs, F. Keil, H. Lischka, W. Kutzelnigg, and V. Staemmler, *J. Chem. Phys.*, **63**, 455 (1975).
(23) R. Ahlrichs, H. Lischka, B. Zurawski, and W. Kutzelnigg, *J. Chem. Phys.*, **63**, 4685 (1975).
(24) L. Pauling, "The Nature of the Chemical Bond", 3rd ed, Cornell University Press, Ithaca, N.Y., 1960, p 224.
(25) L. E. Sutton, "Tables of Interatomic Distances and Configuration in Molecules and Ions", The Chemical Society, London, 1958/1965.
(26) F. Driessler, R. Ahlrichs, V. Staemmler, and W. Kutzelnigg, *Theor. Chim. Acta*, **30**, 315 (1973)
(27) B. Zurawski, R. Ahlrichs, and W. Kutzelnigg, *Chem. Phys. Lett.*, **21**, 309 (1973).
(28) F. Ramirez and S. Dershowitz, *J. Org. Chem.*, **22**, 41 (1957).
(29) F. Ramirez and St. Levy, *J. Am. Chem. Soc.*, **79**, 67 (1957).
(30) A. W. Johnson, *J. Org. Chem.*, **24**, 282 (1959).
(31) M. Gelus, R. Ahlrichs, V. Staemmler, and W. Kutzelnigg, *Chem. Phys. Lett.*, **7**, 503 (1970).
(32) C. A. Coulson, "Valence", Oxford University Press, London, 1961, p 215.
(33) R. S. Mulliken, *J. Chem. Phys.*, **23**, 1833, 1841, 2338, 2743 (1955).
(34) R. S. Mulliken, *J. Chem. Phys.*, **36**, 3428 (1962).
(35) R. F. W. Bader, P. M. Beddal, and P. E. Cade, *J. Am. Chem. Soc.*, **93**, 3095 (1971).
(36) P. Schuster, W. Jakubetz, and W. Marius, *Top. Curr. Chem.*, **60**, 1 (1975).
(37) H. Schmidbaur and W. Tronich, *Chem. Ber.*, **101**, 595 (1968).
(38) F. Keil and W. Kutzelnigg, *J. Am. Chem. Soc.*, **97**, 3623 (1975).
(39) H. Siebert, *Z. Anorg. Allg. Chem.*, **273**, 170 (1953).

Condensation Reactions Involving Carbonium Ions and Lewis Bases in the Gas Phase. Hydration of the *tert*-Butyl Cation

K. Hiraoka and P. Kebarle*

Contribution from the Chemistry Department, University of Alberta, Edmonton, Alberta, Canada T6G 2E1. *Received July 6, 1976*

Abstract: The gas-phase reactions $R^+ + OH_2 = ROH_2^+$ where R = s-$C_3H_7^+$ and t-$C_4H_9^+$ lead to protonated 2-propanol and protonated *tert*-butyl alcohol. Proof for this is given by comparing the heats of formation of the ROH_2^+ species obtained as above with those obtained by protonation of the corresponding alcohols. The reactions of alkyl carbocations with n-donor bases like OH_2, CH_3OH, NH_3, CH_3NH_2, etc., probably lead to the corresponding protonated alcohols, ethers, primary amines, secondary amines, etc., and represent a general class of ion–molecule condensation reactions. Condensation reactions of this type and other oligo condensation reactions occur readily in methane containing CO, H_2O, and NH_3 and must be considered, if the importance of ion–molecule reactions to prebiotic synthesis is to be assessed. The energies released in the hydration of the *tert*-butyl$^+$ and protonated *tert*-butyl alcohol, obtained by measurement of the corresponding equilibria, show an interesting pattern: $C_4H_9^+ + OH_2 = C_4H_9OH_2^+$, $-\Delta H$ = 11.2 kcal/mol; $C_4H_9(OH_2)_2^+ + OH_2 = C_4H_9(OH_2)_3^+$, $-\Delta H$ = 17.7 kcal/mol; $C_4H_9(OH_2)_3 + OH_2 = C_4H_9(OH_2)_4^+$, $-\Delta H$ = 14.0 kcal/mol. The low exothermicity of the first reaction is considered to be due to a shift of positive charge from the methyl groups to the OH_2 group which makes the stabilization due to the methyl substituents much less important for the protonated butanol. The conversion of the $C_4H_9OH_2^+$ hydrates to isobutene by the reaction $C_4H_9(OH_2)_n^+ + OH_2 = i\text{-}C_4H_8 + H^+(H_2O)_{n+1}$ was also observed. This reaction is analogous to acid-catalyzed dehydration of alcohols in solution. Thermochemical information for some of the observed reactions is provided.

The present work deals with experimental studies of gas-phase condensation reactions involving alkyl carbocations R^+ and Lewis bases. The reactions occur in a "high pressure" ion source using electron pulses for ionization and operating at a few Torr of pressure. The reactions are followed by mass spectrometric detection of the ions. Equations 1–4 illustrate